Journal of the European Ceramic Society **18** (1998) 813–820

PII: S0955-2219(97)00182-9
0955-2219/98/$19.00 + 0.00

Microstructural Evolution in Self-forming Spinel/Calcium Aluminate-Bonded Castable Refractories

M. Fuhrer,* A. Hey† and W. E. Lee

Department of Engineering Materials, University of Sheffield, UK

(Received 19 August 1997; accepted 22 October 1997)

Abstract

Calcium aluminate bonded alumina-spinel castable refractories have been fabricated with in-situ spinel formation. Spinel formation occurs between 1200 and 1400°C with a net-like morphology interlinked with CaO–MgO–Al_2O_3–SiO_2 phases. Spinel generated at 1400°C is nearly stoichiometric but at higher temperatures it progessively enriches in Al_2O_3. The calcium aluminate phases in the cement bond react to form platey CA_6 crystals between 1200 and 1400°C which coexist with the spinel and penetrate and bond to tabular alumina grains. The potential effect of these morphologies on properties is discussed. © *1998 Elsevier Science Limited. All rights reserved*

1 Introduction

Monolithic calcium aluminate (CA)-bonded refractory castables containing magnesium aluminate spinel are being used increasingly in steelmaking applications such as the linings of steel ladles, continuous casting tundishes and degasser snorkels and lances.[1] The addition of spinel to castable compositions improved slag corrosion and erosion resistance[2–4] and *preformed/prereacted/presynthesised* (sintered or fused) spinel has been used extensively as a grain phase. The MgO–Al_2O_3 binary phase diagram reveals that spinel forms a solid solution with both MgO and Al_2O_3 at high temperatures although it also indicates that these solid solutions are metastable at room temperature so that the cooling rate from the sintering or fusion temperature is an important variable in prereacting spinel material and as a consequence most commercial spinels contain some second phase. Alumina-rich spinels are generally used in steelmaking applications and, in particular, in castable systems where the elimination of free MgO is imperative as this would otherwise react with the water additive and affect the hydration reactions critical to the successful installation of the castable.[5] The presence of free alumina can also improve the thermal shock resistance of the system since the thermal expansion mismatch between the Al_2O_3 (9×10^{-6}/K at 1500°C) and spinel (10.2×10^{-6}/K at 1500°C) leads to a stress state which aids crack closure or generates microcracks.[6] When above-stoichiometric alumina is present in the spinel phase (i.e. the alumina is not present as a free second phase) it decreases the spinel lattice parameter which can thus be used to estimate the extent of non-stoichiometry.[7–9] The microstructure of an alumina-rich spinel/alumina grain castable[10] after firing at 1500°C contains spinel, corundum and calcium hexaluminate, CA_6, derived from the calcium aluminate cement, the latter with a hexagonal, tabular, platey, morphology interlocked with the corundum. This morphology was also seen by Korgul *et al.*[11] at the slag–refractory interface in a corroded spinel-containing castable of similar composition. In a spinel-free, CA-bonded, high alumina castable a similar CA_6 morphology was detected in the matrix although the bonding between CA_6 and tabular alumina was less interlocked and the CA_6 crystals were larger.[10] CA_6 is known to form at temperatures > 1300°C in CA-bonded systems[12] and the processing conditions such as curing temperature are known to influence the CA_6 crystal size and the physical properties of the product.[13] For example, increasing curing temperature from 10 to 30°C gave a finer (about 3 μm compared to 5 μm) CA_6 crystal size resulting in a 15% reduction in corrosive wear rate.

*On secondment from Montanuniversitat Leoben, Austria.
†Also KSR International Ltd., Beauchief, Sheffield, UK.

At high (1670–1700°C) temperatures and long holding times spinel *grain* aggregate castable systems show evidence of 'cracking and peeling'[2] so that new compositions have been developed in which the spinel is generated in service during heating to the use temperature (so-called in situ or self-forming spinels). The spinel in this case is generated by reaction of fine periclase (MgO) additions with alumina present in the *matrix* (bond) fines, often in the CA cement. Self-forming spinel systems often have better resistance to slag penetration and corrosion[14] believed due to greater firing shrinkage and consequent higher density in the product. Creep manifest by 'peeling' (i.e. spalling) of the castable at high temperature (1450°C), and arising from formation of liquid by reaction of the fine silica added to facilitate spinel formation via the liquid, can apparently be controlled by adjustment of the SiO_2/MgO content in the matrix.[14] Bier *et al.*[15] have recently examined the influence of the fine MgO on rheology and hydration in Ca-based castables.

However, microstructural studies of spinel formation in the matrix of calcium aluminate castables have not been performed so that understanding of the formation mechanism is limited. The purpose of the present study was to determine, from a detailed microstructural study, the nature of *in-situ* spinel formation in the matrix of these systems as well as the morphologies of other phases present such as CA_6 and $CaO\text{-}MgO\text{-}Al_2O_3\text{-}SiO_2$ phases and their interaction with the matrix spinel and the alumina grain.

2 Experimental

One castable formulation was prepared from tabular alumina (TA) grain and a matrix derived from fine tabular alumina, high alumina cement (HAC), reactive calcined alumina, microsilica and seawater derived MgO (Table 1). The raw materials were mixed in a Hobart mixer for 5 min with 6.5 wt% water. The resulting slip was cast into 7·6×7·6×7·6 cm plastic moulds and the concrete allowed to hydrate under ambient conditions for 16 h. The cubes were dried for a further 16 h at 110°C and subsequently fired for 3 h at 1200, 1400 and 1600°C in air in an electric chamber furnace. The sintering profiles of the samples denoted SF 1200, SF 1400 and SF 1600 are given in Fig. 1. Samples for X-ray powder diffraction (XRD) analysis were taken from crushed and sieved ($< 250\,\mu m$) cubes and diffractograms recorded on a Philips PW1050 unit using Ni-filtered CuK_α radiation operating at 30mA and 40kV. JCPDS cards 21–1152 ($MgAl_2O_4$ spinel), 10–173 (α-Al_2O_3 corundum), 21–2095 (β'-$NaAl_7O_{11}$), 4–829 (MgO periclase) and 25–122 ($CaAl_{12}O_{19}$, CA_6, hibonite) were used for phase identification. Semi-quantitative phase contents were determined using integrated XRD peak intensities (Table 2). Samples for microstructural analysis were taken from the cube corners and the inside surfaces (at a depth of about 1 cm) were examined. Standard ceramographic mounting, grinding and polishing techniques were used[16] and all samples were carbon coated before analysis in a Camscan Series 2 scanning electron microscope (SEM) equipped with a Link AN10000 energy dispersive spectroscopy (EDS) system. Both secondary electron imaging (SEI) and backscattered electron imaging (BEI) was used.

Table 1. Castable formulation

Constituent	*Content (wt%)*
Aggregates:	
Tabular alumina > 250 μm	70
Matrix:	
Tabular alumina < 250 μm	12
High alumina cement	5
Reactive alumina < 10 μm	3·5
Micro silica < 10 μm	1
Seawater magnesia < 250 μm	8·5

3 Results and Discussion

3.1 Phase evolution

XRD patterns of SF 1200, SF 1400 and SF 1600 are given in Fig. 2(a)–(c); the phase compositions and contents estimated from the peak intensities are given in Table 2. Spinel is present in all samples, although after firing at 1200°C the content was low at ≈8%. However, after firing at 1400 and 1600°C the spinel constitutes the main phase so that the main spinel formation seems to occur between 1200 and 1400°C. This is supported by the fact that only at 1200°C was free periclase detected [Fig. 3(a)]. The large amount of free corundum in all samples is due to the tabular alumina aggregates which form the bulk of the castable. However, the corundum content decreases rapidly with increasing temperature (Table 2). This is due both its *reaction* with periclase to form spinel and its *dissolution* in the spinel generated (see below).

At 1200°C a significant number of small, unidentified peaks were present [Fig. 2(a)]. The composition of the castable however suggests that they are mainly due to the CaO-containing phases of the cement. A wide variety of possible CA phases may be present at this temperature since no equilibrium is established. Moreover the free SiO_2 may have formed $CaO\text{–}Al_2O_3\text{–}SiO_2$ (CAS), CaO–MgO–

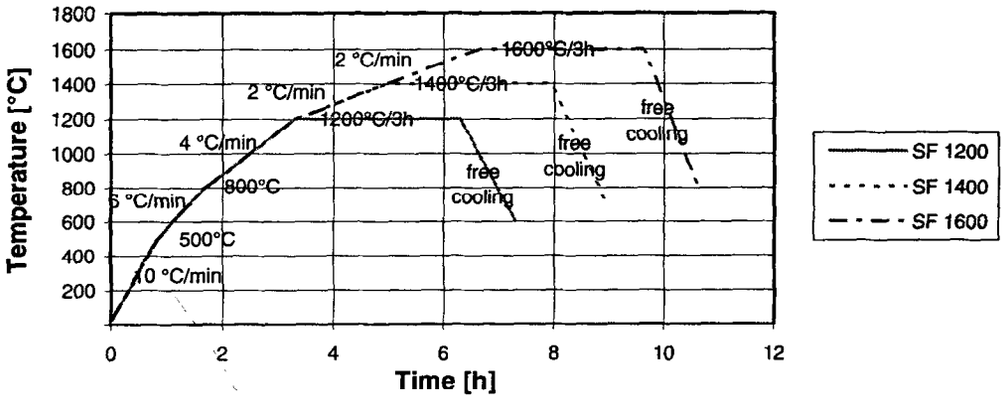

Fig. 1. Sintering profiles for self-forming spinel castables.

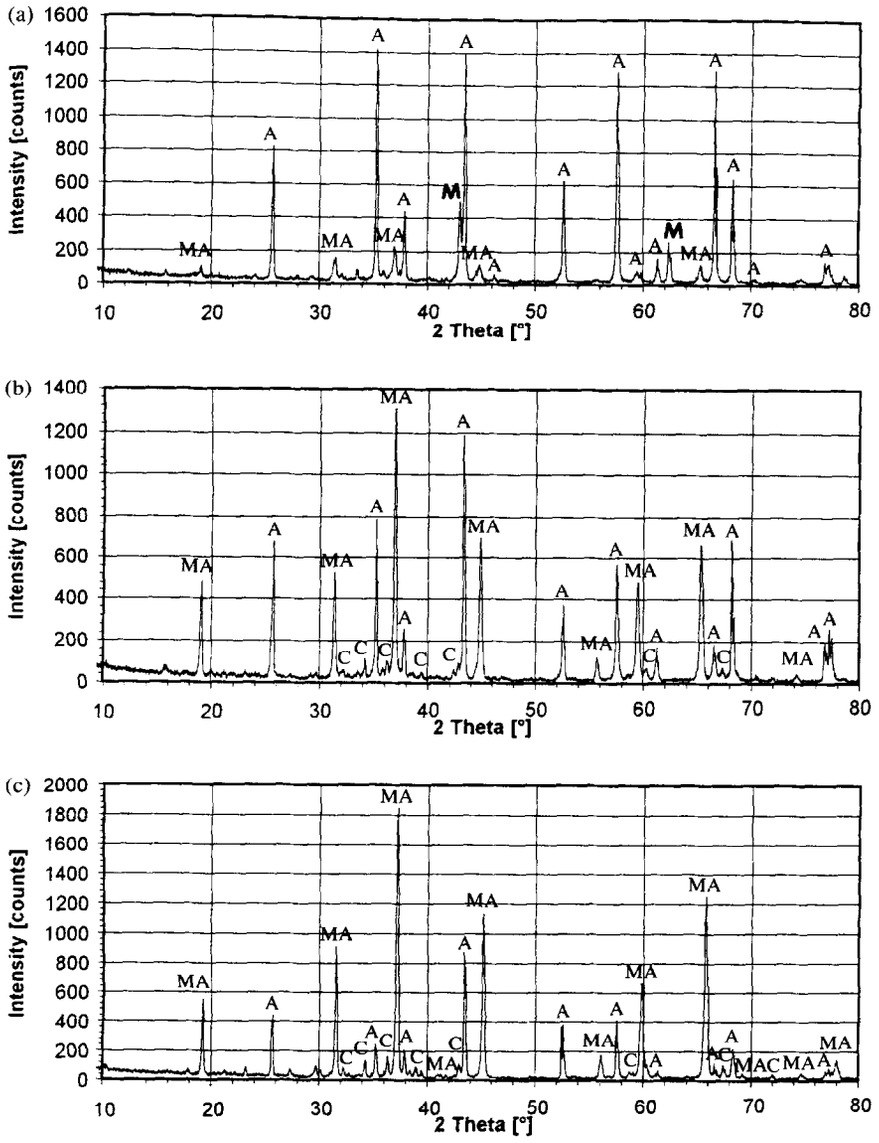

Fig. 2. XRD spectra for (a) SF 1200, (b) SF 1400 and (c) SF 1600. M = MgO, A = α-Al_2O_3, MA = magnesium aluminate spinel, C = $CaAl_{12}O_{19}$.

SiO_2 (CMS) or CaO–MgO–Al_2O_3–SiO_2 (CMAS) phases which have various stoichiometries. At 1400 and 1600°C, however, CA_6 is clearly identified and the quantity of unidentified phases decreased [Fig. 2(b) and (c)]. Due to the high overall Al_2O_3 content for the castable the presence of this phase at elevated temperatures is in accord with the CaO–Al_2O_3 phase diagram.

The lattice parameters of the spinel show a clear decrease between 1400 and 1600°C (Table 3).

Table 2. Phase compositions and contents determined from XRD peak intensities

Sample name	*Major phase content (wt%)*	*Minor phase content (wt%)*	*Additional phases (wt%)*
TA 60	Corundum 93	NA_7 7	
SF 1200	Corundum 64	Periclase 22	Spinel 8, unidentified 6
SF 1400	Spinel 50	Corundum 45	CA_6 3; unidentified 2
SF 1600	Spinel 66	Corundum 27	CA_6 5; unidentified 2

Table 3. Lattice parameters of spinel and corundum phases

Sample name	*Lattice parameters*		
	Spinel: a (Å)	*Corundum: a (Å)*	*Corundum: c (Å)*
TA 60	—	4·760	12·999
SF 1200	8·072	4·752	12·991
SF 1400	8·071	4·758	12·996
SF 1600	8·028	4·756	12·987

Comparing the lattice parameters with literature values[8,9] suggest the MA spinel at 1200 and 1400°C contains 73% Al_2O_3. However, from 1400 to 1600°C the spinel enriches in alumina up to 83%. This dissolution reaction explains why the quantity of corundum phase in the castable still decreased between 1400 and 1600°C (Table 2) although no free MgO was present to react above 1200°C.

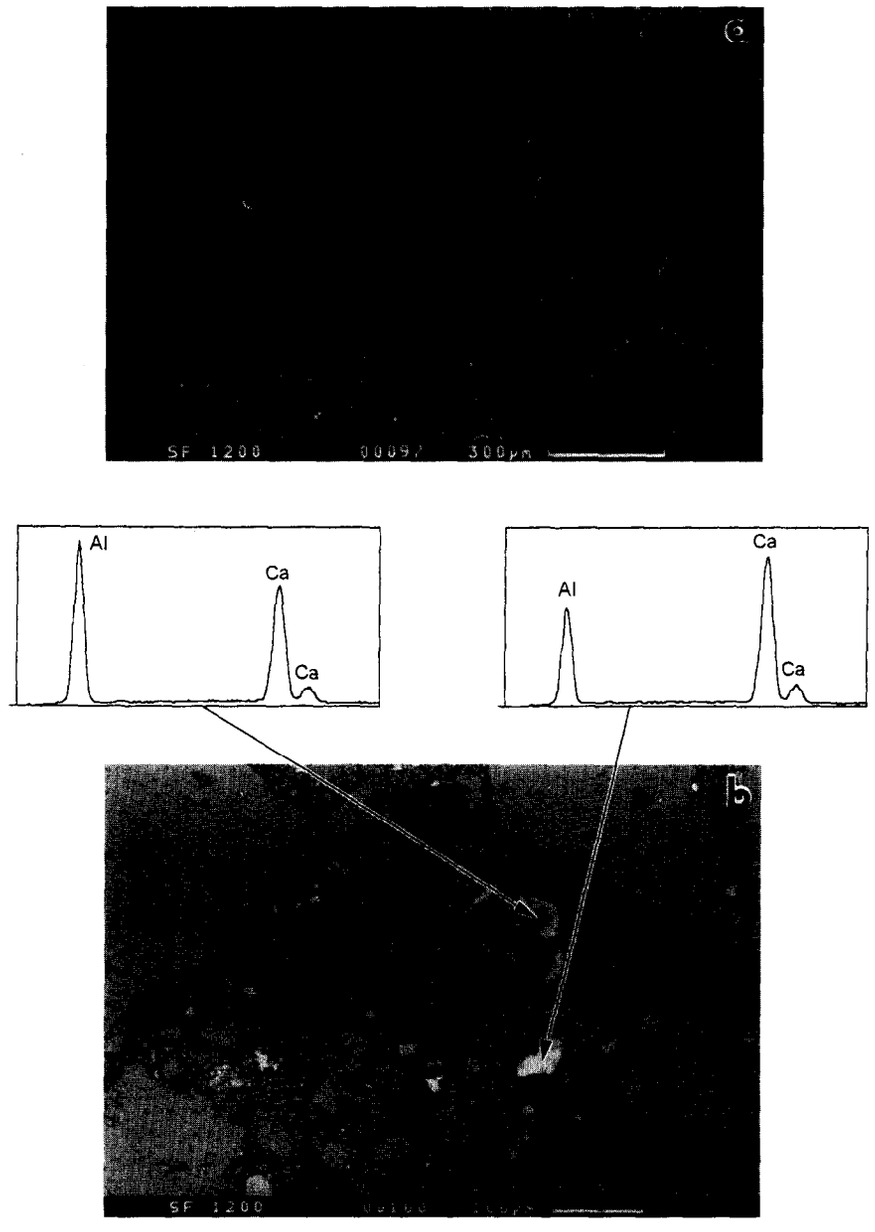

Fig. 3. Matrix/bond microstructure in SF 1200, (a) SEI and (b) BEI with EDS analysis.

3.2 Phase morphology

XRD indicates little spinel formation in SF 1200, the main phases being corundum and periclase. Figure 3(a) is an SEI image which reveals the matrix and the fine dark, porous, tabular alumina grain which does not appear to have reacted at this temperature. The slightly smaller and brighter, grey grains are periclase which can be distinguished from the tabular alumina also by their lower porosity. In the BEI image Fig. 3(b) the tabular alumina is brighter (medium grey) than the periclase (dark grey) and the whitest grains are various CA compositions as shown by EDS. The finest particles in the matrix occupying the space between the medium sized particles have formed necks and bridges with adjacent fine particles (Fig. 4). This fine matrix has various compositions in the CA and CAS system and these bridges and links constitute the cement binding phase. The liquid phase sintering additives could be detected in the sea water derived MgO as light CMS phases (Fig. 5).

By 1400°C no free periclase was found confirming the results of the XRD. The alumina grains are no longer clearly separated from the matrix as at 1200°C. Rather, the matrix has formed a *net-like structure* which links the remaining alumina grains. Figures 6 and 7 show that the matrix structure is similar to that observed for SF 1200 where it was identified as CA/CAS phases (Fig. 4). However, EDS shows that the small links and bridges in this net have additionally dissolved some MgO and are now compositions in the CMAS system. Moreover the tuber-like junctions in this net are pure MA spinel, which is intensively bonded to the CMAS net. The third phase detected consists of small ($\approx 10\,\mu m$ long by $\approx 2\,\mu m$ wide) CA_6 crystals which, in the matrix, can mainly be found in clusters or on the surface of TA grains (Fig. 8). The CA_6 crystals form also in the interior of the tabular alumina, particularly in the regions close to the surface. Consequently, the CA_6 bonds the grains and the matrix.[10] However, CA_6 also starts to form

Fig. 4. SEI of the fine structure of the matrix in SF 1200.

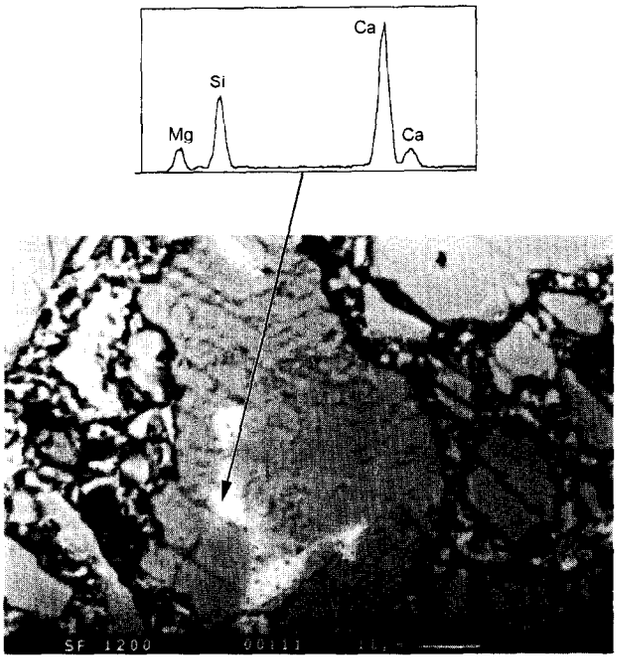

Fig. 5. BEI and EDS of the CMS bond phase in seawater–MgO.

Fig. 6. SEI of the matrix in SF 1400.

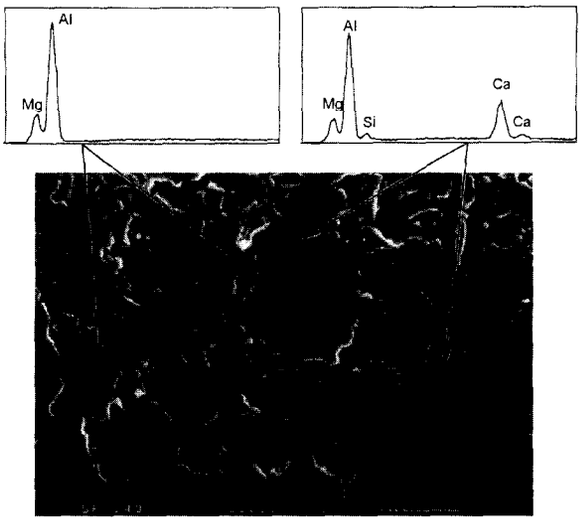

Fig. 7. SEI and EDS of the spinel/CMAS net in SF 1400.

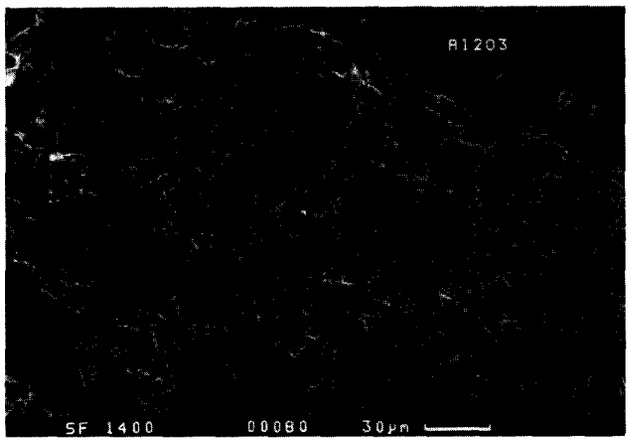

Fig. 8. CA_6 clusters in SF 1400 (SEI).

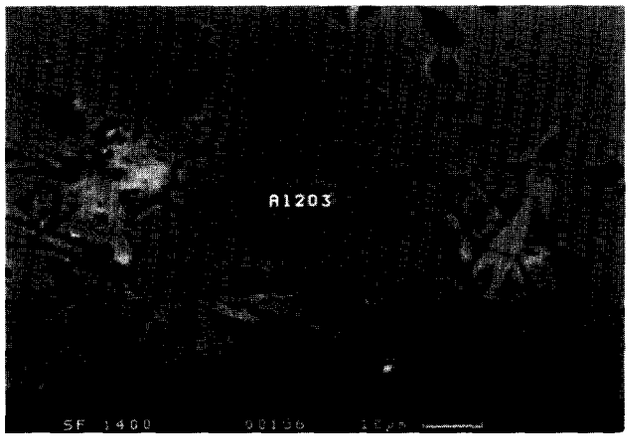

Fig. 9. CA_6 formation in the interior of tabular alumina grain (BEI).

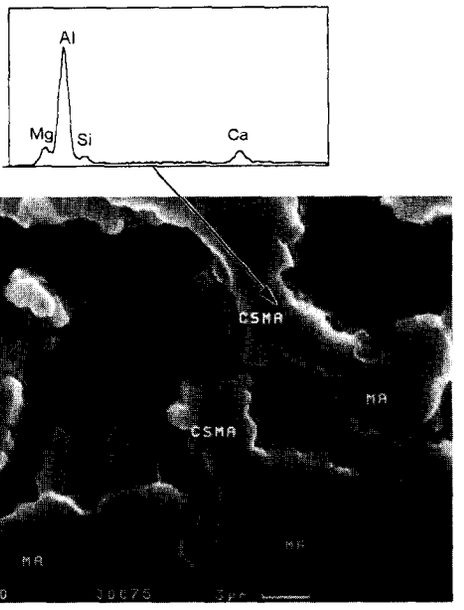

Fig. 10. Detail of the net in SF 1600 (cf. Fig. 7).

Fig. 11. Cluster of CA_6 needles in SF 1600 (SEI).

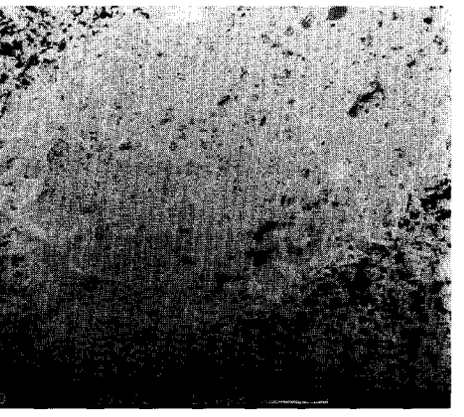

Fig. 12. Extensive CA_6 needle penetration in tabular alumina grain (BEI).

in the pores of the grain interiors (Fig. 9). This suggests that rapid grain boundary diffusion or vapour transport processes have taken place. The CA_6 crystals which form in the interior of the tabular alumina moreover appear to open up the alumina grains although this process is much more obvious at 1600°C.

The microstructure of the castable fired at 1600°C is similar to that of the castable fired at 1400°C, although more advanced. The net-like matrix has a similar structure although the CMAS bridges contain less CaO (Fig. 10). The CA_6 crystals in the matrix also have a similar distribution as in SF 1400 although they are longer [$\approx 30\,\mu$m by $\approx 5\,\mu$m (Fig. 11)]. The most significant difference to the 1400°C castable seems to be the progress of CA_6 penetration into Al_2O_3 grains. Figure 12 shows CA_6 in a large tabular alumina grain. The structure of the alumina is clearly less dense than at 1200 and 1400°C as a result of the CA_6 penetration. In particular, most of the CA_6 is close to the alumina grain surface forming a network structure pushing into the grain. Large differences in the molar volumes of CA_6 and Al_2O_3 lead to large stresses being generated as the CA_6 forms and to the opening up of the Al_2O_3 grain.[17]

Figure 13(a)–(c) shows alumina grains at different stages of structure loosening. In Fig. 13(c) the original grain has almost completely disintegrated. It should be noted that few (< 5% of the total

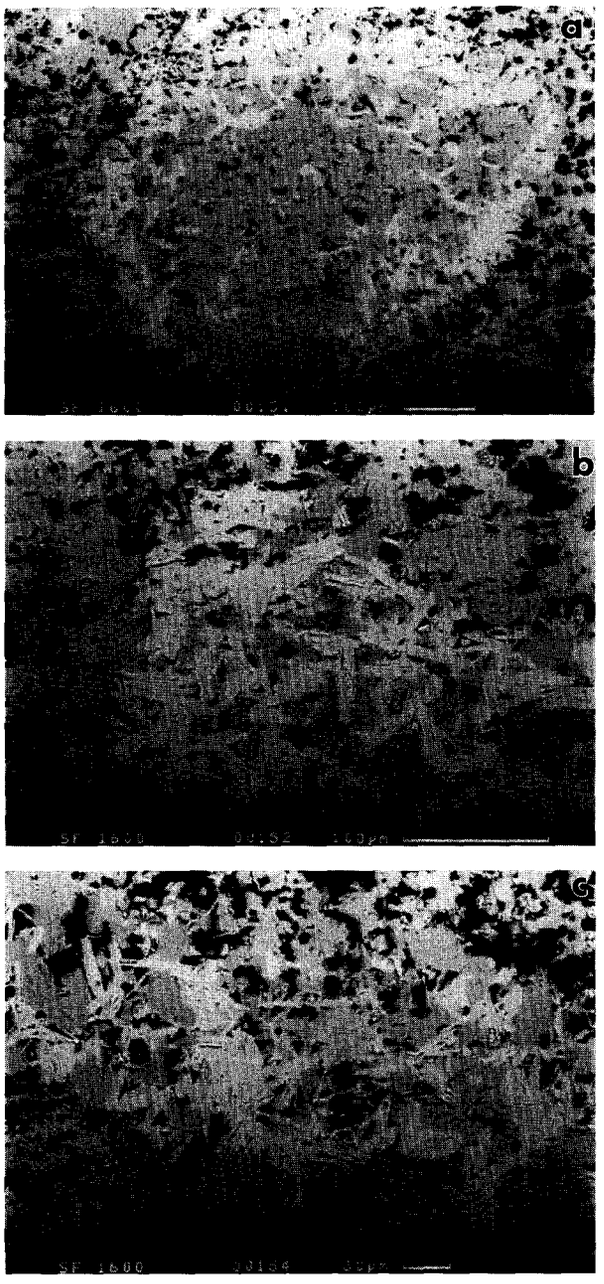

Fig. 13. Increasing tabular alumina grain loosening (a) to (c) due to CA_6 penetration in SF 1600.

volume) remnant tabular alumina grains were found probably due to their dissolution in the spinel explaining the sharp decrease in the spinel lattice parameter from 1400 to 1600°C (Table 3). This dissolution may also be a driving force for the structure loosening of the alumina since the generated spinel was not saturated in alumina at 1400°C and was therefore far from equilibrium. It should also be noted that only about a half of the alumina grains were affected by the CA_6 penetration.

The influence of these microstructural observations on the properties of the resulting castable will now be briefly considered. The interlocked CA_6 plates and contiguous net structure of the spinel-rich matrix might give rise to the known good thermal shock resistance since they would provide toughening mechanisms such as crack bridging and deflexion. The in-situ spinel might be expected to have a greater surface area than pre-reacted material and so contribute more to the corrosion resistance by accommodating, for example, Mn and Fe from the slag. The slag resistance mechanism is believed[11] to be associated with the spinel accepting such ions from the slag so raising its viscosity and limiting penetration. On the other hand the opening up (loosening) of the tabular alumina grain and the resulting cracks in them from CA_6 penetration might be expected to result in an enhanced slag penetration and a decreased mechanical strength. Conversely, the greater bonding between the matrix and grain associated with the interlocking CA_6 may increase strength. Urita *et al.* [14] found improved slag resistance of self-forming spinel castables associated with increased densities with spinel present. It is possible that the sample density is higher while the isolated grain densities are reduced due to greater sintering of the spinel containing continuous bond phase. Physical and thermomechanical property and slag testing results on these castables will be the subject of a future publication.

4 Conclusions

- In self-forming spinel castables spinel formation occurs between 1200 and 1400°C with a contiguous net-like matrix morphology linked with CMAS phases.
- At 1400°C the spinel generated is nearly stoichiometric but on heating to 1600°C it enriches in Al_2O_3 from 73% up to 83%.
- The CA phases of the cement bond convert into CA_6 crystals between 1200 and 1400°C which penetrate tabular alumina grains leading to complete disintegration of up to a half of the alumina grain.

References

1. Hey, A., Gregory, S. J., Hutchesson, G. S., Pickard, D. M., Taylor, D. S. and Tomlinson, S. B., Applications of engineered castable systems to refractory linings in the steel industry. 39th Int. Coll. on Refr. in "Stahl&Eisen spezial" Vol. 10, 1996 104–107.
2. Mori, J., Toritani, Y. and Tanaka, S., Development of alumina–magnesia castable for steel ladle, in Proc. Unified International Technical Conference on Refractories, UniteCR, 95, Kyoto, Japan, 1995, pp. 171–178.
3. Mori, J., Watanabe, N., Yoshimura, M., Oguchi, Y. and Kawakami, T., Material design of monolithic refractories for steel ladle. *Am. Ceram. Soc. Bull*, 1990, **69**(7), 1172–1176.
4. Nagai, B., Matsumoto, O. and Isobe, T., Development of high-alumina castable for steel ladles. *Taikabutsu Overseas*, 1988, **10**(1), 23–28.

5. Evans, R. M., Magnesia–alumina–spinel. *Am. Ceram. Soc. Bull*, 1993, **72**(4), 59–63.
6. Wilson, D. R., Evans, R. M., Wadsworth, I. and Cawley, J., Properties and applications of sintered magnesia alumina spinels. *Iron & Steel Review*, 1995, **4**, 25–30.
7. Shirasuka, K. and Yamaguchi, G., Precise measurement of the crystal data and the solid solution range of the defective spinel, $MgO.nAl_2O_3$. *Journ. of the Jap. Ceram Soc*, 1974, **82**(12), 34–37.
8. Bailey, J. T. and Russell, R., Preparation and properties of dense spinel ceramics in the $MgAl_2O_4$–Al_2O_3 system. *Trans. Brit. Ceram. Soc*, 1969, **68**, 159–164.
9. Vishnevskii, I. I. and Skripak, V. N., Scattering of phonons by cation vacancies in spinels. *Soviet Physics—Solid State*, 1966, **7**(10), 2374–2377.
10. MacZura, G., Madono, M., Kriechbaum, G. W. and Sewell, B., Low moisture regular corundum/spinel castables with superior properties. Proc. UniteCR 95, Kyoto, Japan, 1995, pp.179–186.
11. Korgul, P., Wilson, D. R. and Lee, W. E., Microstructural analysis of corroded alumina–spinel castable refractories. *J. Euro. Ceram. Soc*, 1997, **17**, 77–84.
12. Givan, G. V., Hart, R. D., Heilich, R. P. and MacZura, G., Curing and firing high purity calcium aluminate–bonded tabular alumina castables. *Am. Ceram. Soc. Bull*, 1975, **54**(8), 710–713.
13. Adachi, K., Kuwayama, M., Yoshida, M. and Yamamoto, T., Progress in ladle refractories techniques at Kawasaki Steel, Mizushima Works. in Proc. Unified International Technical Conference on Refractories, UniteCR, 95, Kyoto, Japan, 1995, pp. 242–249.
14. Urita, Y., Sugawara, M., Kataoka, M. and Yamaguchi, K., Development of self-forming spinel castable for steel ladle, 39th Int. Coll. on Refr, in "Stahl&Eisen spezial", Vol. 10, 1996, pp. 108–111.
15. Bier, T. A., Parr, C., Revais, C. and Fryda, H., Chemical interactions in calcium-aluminate cement based castables containing magnesia, Proc. Unified International Technical Conference on Refractories, UniteCR, New Orleans, LA, *Am. Ceram. Soc.*, 1997, pp. 15–21.
16. Lee, W. E. and Rainforth, W. M., Ceramic microstructures—property control by processing, Chapman & Hall, London, 1994.
17. Guha, J. P., Reaction chemistry in dissolution of polycrystalline alumina in lime-alumina-silica slag. *Brit. Ceram. Trans.*, 1997, **96**(6), 231–236.